

## 吡啶-3-甲醛缩氨基硫脲合镍(II)、锌(II)配合物的合成、 晶体结构及生物活性

边贺东 李春英 梁宇宁 郭桂全 于 青 梁 宏\*

(广西师范大学化学化工学院, 桂林 541004)

**摘要:** 本文合成并表征了吡啶-3-甲醛缩氨基硫脲(HL)合镍(II)、锌(II)配合物。在配合物 $[\text{NiL}_2]$  (1)中, 镍(II)离子与来自 2 个脱氢配体的 2 个氮原子和 2 个硫原子配位, 形成四配位的平面正方形构型。在配合物 $[\text{Zn}(\text{HL})_2(\text{C}_2\text{H}_5\text{OH})_2(\text{H}_2\text{O})_2](\text{NO}_3)_2$  (2)中, 锌(II)离子与 2 个中性配体、2 个乙醇分子和 2 个水分子配位, 配位原子在锌(II)离子周围形成畸变的八面体构型。通过荧光吸收法研究了配合物 1、2 与小牛胸腺 DNA 的作用机理。结果表明, 这 2 个配合物均以插入形式进入 DNA 的碱基对。此外, 还研究了配体及 2 个配合物对金黄色葡萄球菌、乙型溶血性链球菌、肺炎链球菌、炭疽杆菌的抗菌活性。结果表明, 配体及配合物 1 对上述测试菌种无抑制作用, 配合物 2 对前面 3 种有弱的抑菌作用。

**关键词:** 镍<sup>II</sup>配合物; 锌<sup>II</sup>配合物; 氨基硫脲; DNA 作用; 抗菌活性

中图分类号: O614.81\*3; O614.24\*1

文献标识码: A

文章编号: 1001-4861(2008)04-0527-07

## Synthesis, Crystal Structures, and Bioactivities of Ni<sup>II</sup> and Zn<sup>II</sup> Complexes with Pyridine-3-carbaldehyde Thiosemicarbazone

BIAN He-Dong LI Chun-Ying LIANG Yu-Ning GUO Gui-Quan YU Qing LIANG Hong\*

(College of Chemistry and Chemical Engineering, Guangxi Normal University, Guilin, Guangxi 541004)

**Abstract:** The Ni<sup>II</sup> and Zn<sup>II</sup> complexes with pyridine-3-carbaldehyde thiosemicarbazone (HL) have been synthesized and characterized by X-ray diffraction. In the  $[\text{NiL}_2]$  (1), the Ni<sup>II</sup> atom was four-coordinated to form a square geometry by two nitrogen atoms and two sulfur atoms from two different deprotonated ligands. In  $[\text{Zn}(\text{HL})_2(\text{C}_2\text{H}_5\text{OH})_2(\text{H}_2\text{O})_2](\text{NO}_3)_2$  (2), the Zn<sup>II</sup> atom was in a distorted octahedral geometry coordinated by two neutral ligands, two ethanol molecules, and two water molecules. The binding of the two complexes with calf thymus DNA has been investigated by absorption, luminescence titrations. The results suggest that both the two complex intercalates into DNA base pairs. Antimicrobial activities of the free ligand and the two complexes against *Staphylococcus Aureus*,  *$\beta$ -hemolytic streptococcus*, *Streptococcus Pneumoniae*, *Bacillus Anthracis* shows that the free ligand and 1 did not inhibit the growth of the test microorganisms and 2 showed weak activities against the three former tested microorganisms. CCDC: 288409, 1; 288410, 2.

**Key words:** Ni<sup>II</sup> complex; Zn<sup>II</sup> complex; thiosemicarbazone; DNA binding; antimicrobial activities

Thiosemicarbazones are particular interest because of their versatility towards different metal ions either as a neutral ligand or as a deprotonated ligand

through the S, N, N atoms<sup>[1-3]</sup>. Furthermore, thiosemicarbazones and their complexes have demonstrated significant biological activity and new examples are

收稿日期: 2007-10-10。收修改稿日期: 2008-01-22。

教育部高校青年教师奖资助项目, 广西师范大学博士启动基金。

\*通讯联系人。E-mail: gxnuchem312@yahoo.com.cn

第一作者: 边贺东, 男, 33 岁, 教授; 研究方向: 配位化学、生物无机化学。

being tested for their antitumor, antimicrobial, and antiviral activity<sup>[4-12]</sup>. Biological activities of the metal complexes differ from those of either the ligand or the metal ion itself, and increased and/or decreased biological activities are reported for several transition metal complexes such as copper(II) and nickel(II)<sup>[13]</sup>.

The biological activity is considered to involve three kinds of mechanisms: (i) inhibition of the enzyme ribonucleoside diphosphate reductase (essential for DNA synthesis)<sup>[14]</sup>; (ii) creation of lesion in DNA strands by oxidative rupture<sup>[15]</sup>; (iii) binding to the nitrogen bases of DNA or RNA, hindering or blocking base replication<sup>[16]</sup>. In order to learn the relationship between the biological properties and the structures of metal complexes, it is necessary to study the interaction between them and DNA. In this paper, the Ni<sup>II</sup> and Zn<sup>II</sup> complexes with pyridine-3-carbaldehyde thiosemicarbazone (HL) have been synthesized and characterized by X-ray diffraction crystal structure analysis. The interactions of the two complexes and DNA and antimicrobial activities were studied.

## 1 Experimental

### 1.1 Materials

Thiosemicarbazide, Zn(NO<sub>3</sub>)<sub>2</sub>·6H<sub>2</sub>O, Ni(OAc)<sub>2</sub>·2H<sub>2</sub>O, Pyridine-3-carbaldehyde, were purchased from commercial source. The ligand HL was prepared using the published procedure<sup>[17]</sup>. Calf thymus DNA (CT-DNA) was purchased from the Huamei Biotechnology Company (China). The spectroscopic titration was carried out in the buffer (5 mmol·L<sup>-1</sup> Tris-HCl, 50 mmol·L<sup>-1</sup> NaCl, pH 7.4) at room temperature. A solution of CT-DNA in the buffer gave the ratio of UV absorbance at 260 and 280 nm,  $A_{260}/A_{280}$ , of *ca.* 1.8~1.9:1, which indicated that the DNA was sufficiently free of protein<sup>[18]</sup>. The DNA concentration per nucleotide was

determined by absorption spectroscopy using the known molar extinction coefficient value of 6 600 L·mol<sup>-1</sup>·cm<sup>-1</sup> at 260 nm<sup>[19]</sup>.

### 1.2 Synthesis of complex [Ni(C<sub>7</sub>H<sub>7</sub>N<sub>4</sub>S)<sub>2</sub>] (1)

The mixture of pyridine-3-carbaldehyde thiosemicarbazone (0.6 mmol), Ni(OAc)<sub>2</sub>·2H<sub>2</sub>O (0.3 mmol), C<sub>2</sub>H<sub>5</sub>OH (8 mL) and CH<sub>3</sub>CN (8 mL) was stirred evenly and was placed in a 20 mL stainless-steel bomb at 110 °C. After 3 days, the temperature was decreased to 20 °C and the dark-green crystals were obtained. Anal. Calc for C<sub>14</sub>H<sub>14</sub>N<sub>8</sub>NiS<sub>2</sub> (%): C 40.27; H 3.36; N 26.85; S 15.34 and Found (%): C 40.12; H 3.25; N 26.58; S 15.48.

### 1.3 Synthesis of complex [Zn(C<sub>7</sub>H<sub>8</sub>N<sub>4</sub>S)<sub>2</sub>(H<sub>2</sub>O)<sub>2</sub>(C<sub>2</sub>H<sub>5</sub>OH)<sub>2</sub>](NO<sub>3</sub>)<sub>2</sub> (2)

Zn(NO<sub>3</sub>)<sub>2</sub>·6H<sub>2</sub>O (1 mmol) was added to a 20 mL ethanol solution of the ligand (1 mmol). After refluxed for 1 h, the mixture was cooled to room temperature and filtered. The filtrate was slowly evaporated at room temperature. After two weeks, good quality yellow crystals were obtained and were suitable for X-ray structure determination. (Anal. Calc. for C<sub>18</sub>H<sub>32</sub>N<sub>10</sub>O<sub>10</sub>S<sub>2</sub>Zn (%): C 40.71; H 4.72; N 20.65; S 9.44 and Found (%): C 40.50; H 4.55; N 20.35; S 9.78.

### 1.4 Crystal structure determination

Single crystal X-ray diffraction data collection were performed on a Bruker Smart 1000CCD diffractometer with Mo K $\alpha$  radiation ( $\lambda=0.071\ 073$  nm). Absorption effects were corrected by semi-empirical methods. The structures were solved by direct methods with the program SHELXS-97<sup>[20]</sup> and refined with SHELXL-97<sup>[21]</sup>. The non-hydrogen atoms were located by direct phase determination and difference Fourier syntheses, and refined by full-matrix least-squares methods on  $F^2$ , while the hydrogen atoms for non-water protons were treated using the riding model. Further details of the structural analyses are summarized in Table 1.

Table 1 Crystal data and structure parameters for the complex 1 and 2

	1	2
Empirical formula	C <sub>14</sub> H <sub>14</sub> N <sub>8</sub> NiS <sub>2</sub>	C <sub>18</sub> H <sub>32</sub> N <sub>10</sub> O <sub>10</sub> S <sub>2</sub> Zn
Formula weight	417.16	678.03
Temperature / K	293(2)	293(2)
Wavelength / nm	0.071 073	0.071 073
Crystal system	Monoclinic	Triclinic

Continued Table 1

Space group	$P2_1/c$	$P\bar{1}$
$a$ / nm	0.547 74(16)	0.805 4(3)
$b$ / nm	1.986 5(6)	0.893 6(3)
$c$ / nm	0.753 0(2)	1.120 8(4)
$\alpha$ / (°)		100.682(5)
$\beta$ / (°)	92.340(5)	106.516(5)
$\gamma$ / (°)		104.484(5)
$V$ / nm <sup>3</sup>	0.818 7(4)	0.719 6(4)
Formula units ( $Z$ )	2	1
$D_{\text{calc}}$ / (g·cm <sup>-3</sup> )	1.692	1.565
Absorption coefficient / mm <sup>-1</sup>	1.456	1.066
$F(000)$	428	352
$\theta$ range for data collection / (°)	2.89~25.00	1.97~25.01
$hkl$ ranges	-6~-6, -20~23, -8~8	-9~-5, -9~10, -13~13
Reflections collected	4 226	3 800
Independent reflection ( $R_{\text{int}}$ )	1 443 (0.030 3)	2 533 (0.012 7)
Final $R$ indices [ $I > 2\sigma(I)$ ]	$R_1=0.030$ 3, $wR_2=0.065$ 6	$R_1=0.025$ 4, $wR_2=0.070$ 7
$R$ indices (all data)	$R_1=0.044$ 4, $wR_2=0.069$ 7	$R_1=0.028$ 9, $wR_2=0.073$ 7

### 1.5 Physical measurements

Elemental analyses (C, H and N) was carried out with the America Perkin-Elmer company PE2400 II Element Analyzer. Infrared spectra were performed as KBr pellet using a Perkin-Elmer spectrum one FTIR spectrometer. UV-Vis spectra were recorded on Varian Cary-100 type UV-Spectrophotometer, and emission spectra were recorded on a RF-53019c luminescence spectrometer.

The DNA-binding experiments were performed at room temperature. Absorption titration experiments of the two complexes in buffer were performed by using a fixed metal complex concentration to which increments of the DNA stock solution were added. Complex-DNA solutions were allowed to incubate for 10 min before the absorption spectra were recorded. Fluorescence quenching experiments were conducted by adding small aliquots of the complex solution to the samples containing 5  $\mu\text{mol} \cdot \text{L}^{-1}$  ethidium bromide (EB) and 50  $\mu\text{mol} \cdot \text{L}^{-1}$  DNA in buffer. Samples were excited at 319 nm and emission was observed between 500 and 700 nm.

### 1.6 Determination of antimicrobial activity

Antimicrobial activities were evaluated using the macro dilution test<sup>[22]</sup>. The antibacterial potential of the

ligand and the two complexes was assayed using four positive (*Staphylococcus Aureus*,  $\beta$ -hemolytic *Streptococcus*, *Streptococcus Pneumoniae*, *Bacillus Anthracis*) bacterial strains. The ligand and the two complexes were dissolved in water, and then the minimum inhibitory concentration (MIC) was determined by inhibition of the visible growth of organisms during subsequent incubation for 48 h at 37 °C.

CCDC: 288409, **1**; 288410, **2**.

## 2 Results and discussion

### 2.1 Description of structure

A perspective view of **1** with the atomic numbering scheme is shown in Fig.1. Selected bond lengths and angles are listed in Table 2.

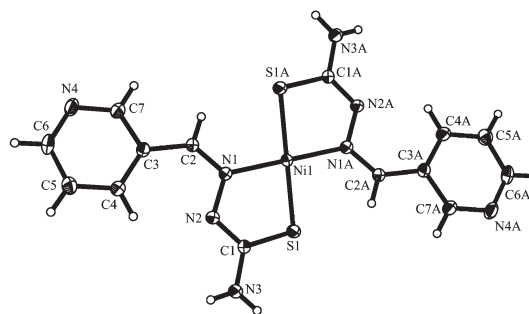


**Table 2** Selected bond lengths and angles for **1** and **2**

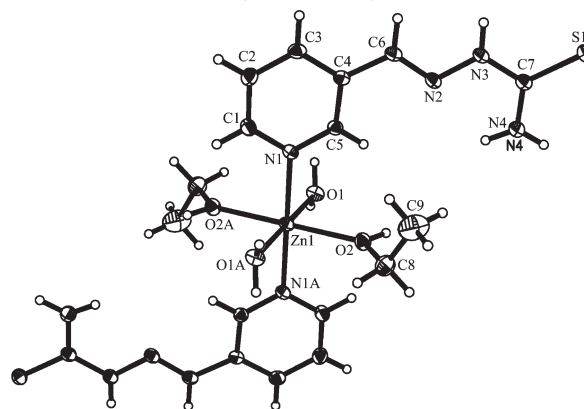
Complex <b>1</b>					
Ni(1)-N(1)	0.191 9(2)	Ni(1)-S(1A)	0.217 44(8)	S(1)-C(1)	0.172 9(3)
Ni(1)-N(1A)	0.191 9(2)	Ni(1)-S(1)	0.217 44(8)		
N(1)-Ni(1)-N(1A)	180.0(1)	N(1)-Ni(1)-S(1)	85.21(6)	S(1A)-Ni(1)-S(1)	180
N(1)-Ni(1)-S(1A)	94.80(6)	N(1A)-Ni(1)-S(1)	94.79(6)		
Complex <b>2</b>					
Zn(1)-O(1)	0.208 27(15)	Zn(1)-O(2)	0.216 65(14)	S(1)-C(7)	0.169 52(19)
Zn(1)-N(1)	0.213 57(16)				
O(1)-Zn(1)-O(1A)	180	O(1)-Zn(1)-O(2)	87.78(5)	N(1)-Zn(1)-N(1A)	180
O(1)-Zn(1)-N(1)	89.61(5)	O(1A)-Zn(1)-O(2)	92.22(5)	N(1)-Zn(1)-O(2)	90.93(6)
O(1A)-Zn(1)-N(1)	90.39(5)	O(1)-Zn(1)-O(2A)	92.22(5)	N(1A)-Zn(1)-O(2)	89.07(6)
O(1)-Zn(1)-N(1A)	90.39(5)	O(2A)-Zn(1)-O(2)	180	N(1)-Zn(1)-O(2A)	89.07(6)

Symmetry transformations used to generate equivalent atoms: complex **1**: A:  $-x+1, -y+1, -z+1$ ; complex **2**: A:  $-x, -y+2, -z+1$ .

This structure consists of the neutral molecules  $[\text{Ni}(\text{L})_2]$  with the metal specify the symmetry centre. The sulphur atom and the hydrazine nitrogen atom of the ligand coordinate to the  $\text{Ni}^{\text{II}}$  atom in a trans configuration to complete a square planar geometry. The torsion angle between the five-membered chelate ring  $\text{Ni1S1C1N2N1}$  and the two thiosemicarbazone moieties is  $9.6^\circ$ , while the dihedral angles between the five-membered chelate ring  $\text{Ni1S1C1N2N1}$  and the pyridyl rings are  $18.1^\circ$ . The distances Ni-S and Ni-N agree well with those generally found in square planar nickel(II) complexes<sup>[23-25]</sup>. Although possessing strong coordination ability, pyridyl N4 atom in the ligand does not coordinate to a  $\text{Ni}^{\text{II}}$  atom as it is participating in a hydrogen bond to  $\text{H3A-N3}$  ( $x-1, -y+3/2, z-1/2$ ) with the  $\text{N4}\cdots\text{N3}$  separation of 0.297 6 nm and the angle of  $161.67^\circ$ . The C1-S1 bond length has been increased from 0.169 3(2) nm in the free protonated ligand<sup>[17]</sup> to 0.172 9(3) nm, confirming that thiol was the major tautomer in **1**. The C1-N2 and C2-N1 distances of 0.130 6(3) and 0.129 3(3) nm, respectively, indicate a electron delocalization in the conjugation of the C-N-N-C moiety in the coordinated ligand.

The structure of **2** contains a two-charged mononuclear cation,  $[\text{Zn}(\text{C}_7\text{H}_8\text{N}_4\text{S})_2(\text{H}_2\text{O})_2(\text{C}_2\text{H}_5\text{OH})_2]^{2+}$ , and two  $\text{NO}_3^-$  anions. A perspective view of the molecular structure is shown in Fig.2. In the cation, the six ligands are arranged around the  $\text{Zn}^{\text{II}}$  ion in a slightly

distorted octahedral geometry, with the metal ion lying on a  $i$  centre. In this description two pyridyl N atoms from different protonated ligands and two ethanol molecules form the equatorial plane while the two water molecules occupy the axial positions at a shorter distance. It is interesting that the S atom of the ligand doesn't coordinate to the centre metal atom. To our knowledge, the sulfur atom bind to  $\text{Zn}^{\text{II}}$  atom in most of cases of  $\text{Zn}^{\text{II}}$  complexes with heterocyclic thiosemicarbazones<sup>[26-30]</sup>. The molecular conformation of the sulfur atom and the hydrazine nitrogen N2 is trans with respect to the C7-N3 bond. The C7-S1 distance (0.169 52(19) nm) is similar to the value in free ligand, which indicate double bond character (thione form).



Symmetry transformations used to generate equivalent atoms:  
A:  $-x, -y+2, -z+1$

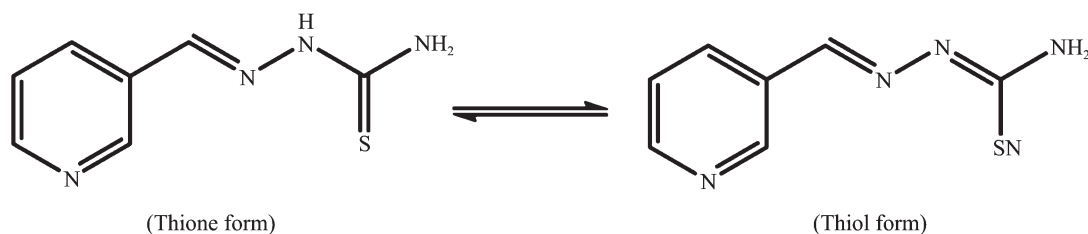
**Fig.2** Molecular structure of **2**

In **2**, O4 from  $\text{NO}_3^-$  anions accepts an intramolec-

ular hydrogen bond from the H2A-O2 with bond distance of 0.281 5 nm and angle of 150.23°. Furthermore, O3 from  $\text{NO}_3^-$  anions acts as an acceptor in hydrogen bonds to N3 ( $-x+1, -y+2, -z+2$ ) and the O1 water molecule ( $-x+1, -y+2, -z+1$ ) with distances of 0.295 9 and 0.281 9 nm, and angles of 163.25° and 165.18°, respectively. These extensive hydrogen bonds also make an important contribution to the stability of the complex.

## 2.2 Infrared spectroscopy

The IR spectra of the ligand L, **1**, and **2** showed



Scheme 1

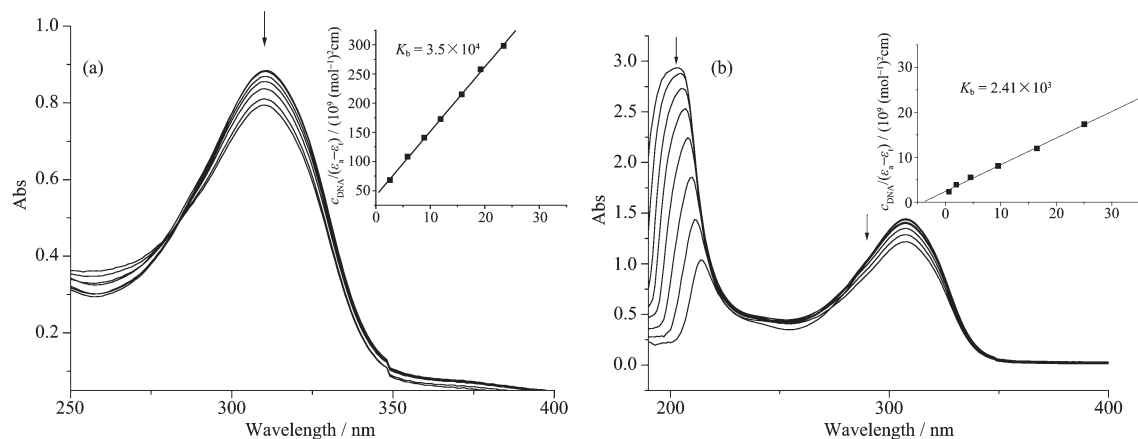
## 2.3 DNA binding studies

### 2.3.1 Absorption spectroscopic studies

The application of electronic absorption spectroscopy in DNA-binding studies is one of the useful techniques. The absorption spectra of these two complexes in the absence and presence of DNA are given in Fig.3. The spectra show one absorption band at 311 nm for **1** and two bands at about 203 and 308 nm for **2**, respectively. With increasing DNA concentrations, there are 11 nm red-shift at 203 nm for **2**, and no obvious red-shift at 311 nm and 308 nm for **1** and **2**,

strong bands in the rang of 3 100~3 500  $\text{cm}^{-1}$ , which are attributed to the  $\nu(\text{N-H})$  mode of the ligand. The bands at 1 628, 1 626, and 1 612  $\text{cm}^{-1}$  in the free ligand, **1**, and **2**, respectively, are contributed to be  $\nu(\text{C=N})$  mode for the Schiff base ligand. The ligand and **2** also showed  $\nu(\text{C=S})$  mode at 1 089 and 1 090  $\text{cm}^{-1}$ , respectively. While the  $\nu(\text{C=S})$  mode disappeared in **1**. The band at 1 032  $\text{cm}^{-1}$  of **1** is attributed to  $\nu(\text{C-S})$  stretching vibrations. These confirm that the ligand has proton adjacent to the thione group in **2**, and trend to turn to the thiol form in **1** (Scheme 1).

respectively, but hypochromicities were observed at the three bands. The band around 310 nm is monitored as a function of added DNA. The binding constant was determined using  $c_{\text{DNA}}/(\varepsilon_a - \varepsilon_f) = c_{\text{DNA}}/(\varepsilon_b - \varepsilon_f) + 1/[K_b(\varepsilon_b - \varepsilon_f)]$ , where  $\varepsilon_a$ ,  $\varepsilon_f$  and  $\varepsilon_b$  correspond to  $A_{\text{obsd}}/c_{\text{complex}}$ , the extinction coefficient for the free complex, and the extinction coefficient of the fully bound complex, respectively. In the plot of  $c_{\text{DNA}}/(\varepsilon_a - \varepsilon_f)$  vs  $c_{\text{DNA}}$ , the binding constant  $K_b$  is given by the ratio of the slope to the intercept. The binding constant for the two complexes are  $3.50 \times 10^4$  and  $2.41 \times 10^3 \text{ L} \cdot \text{mol}^{-1}$  for **1**



Arrow shows the absorbance changes on increasing DNA concentration;  $c_{\text{complex}} = 20 \mu\text{mol} \cdot \text{L}^{-1}$ ,  $c_{\text{DNA}} = 0$  to  $300 \mu\text{mol} \cdot \text{L}^{-1}$

Fig.3 Absorption spectra of **1** (a) and **2** (b) in the presence of increasing amounts of DNA with subtraction of the DNA absorbance

and **2**, respectively, which suggest that there is an interaction between the complexes and DNA.

### 2.3.2 Emission spectra studies

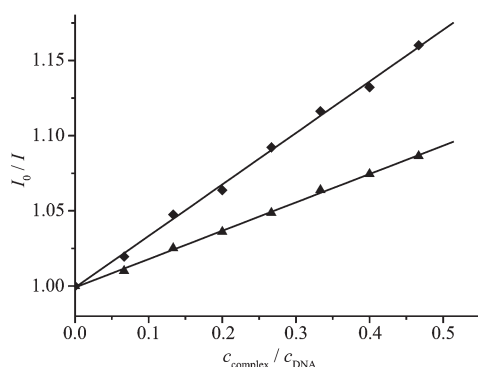
The binding of **1** and **2** to CT-DNA can be studied by competitive binding experiments. Ethidium bromide (EB) is known to show fluorescence when bound to DNA, due to its strong intercalation between the adjacent DNA base pair. The fluorescent light is quenched by the addition of a second molecule<sup>[31,32]</sup>. The quenching extent of fluorescence of EB binding to DNA is used to determine the extent of binding between the second molecule and DNA. The addition of the two complexes to DNA pretreated with EB causes appreciable reduction in the emission intensity, indicating the replacement of the EB fluorophore by the complexes results in a decrease of the binding constant of the ethidium to the DNA.

According to the classical Stern-Volmer equation<sup>[32]</sup>:

$$I_0/I = 1 + Kr$$

where  $I_0$  and  $I$  are the fluorescence intensities in the absence and the presence of complex, respectively.  $K$  is a linear Stern-Volmer quenching constant dependent on the ratio of  $r_{\text{be}}$  (the ratio of the bound concentration of EB to the concentration DNA).  $r$  is the ratio of the total concentration of complex to that of DNA.

The fluorescence quenching curves of EB bound to DNA by the two complexes are shown in Fig.4. The quenching plots illustrate that the quenching of EB bound to DNA by all the complexes are in good agreement with the linear Stern-Volmer equation, which



$c_{\text{EB}} = 5.0 \mu\text{mol} \cdot \text{L}^{-1}$ ,  $c_{\text{DNA}} = 50 \mu\text{mol} \cdot \text{L}^{-1}$ ,  $c_{\text{complex}} = 0$  to  $70 \mu\text{mol} \cdot \text{L}^{-1}$ ,  $\lambda_{\text{ex}} = 319 \text{ nm}$

Fig.4 Fluorescence quenching curves of EB bound to DNA by **1** (■) and **2** (▲)

also indicates that the two complexes binds to DNA. In the plot of  $I_0/I$  vs  $c_{\text{complex}}/c_{\text{DNA}}$ ,  $K$  is given by the ratio of the slope to intercept. The  $K$  values for **1**, **2** are 0.343 1 and 0.188 9, respectively. The data suggest that the interaction of **1** with DNA is stronger than **2**, which is consistent with the above absorption spectral results. However, the smaller  $K$  values indicate that the interaction of the two complexes with DNA is a weak intercalative mode.

### 2.4 Biological activity tests of the complexes

Thiosemicarbazones and their complexes have wide antimicrobial activity. And therefore, we have studied the antimicrobial activities of the free ligand and the two complexes against *Staphylococcus Aureus*,  $\beta$ -hemolytic streptococcus, *Streptococcus Pneumoniae*, *Bacillus Anthracis*. **2** showed weak activities against the tested microorganisms. The MIC against the three former is  $666.7 \mu\text{g} \cdot \text{mL}^{-1}$ , and against the last is larger than  $1000 \mu\text{g} \cdot \text{mL}^{-1}$ . The free ligand and **1** did not inhibit the growth of the test microorganisms. It is also reported that 4-coordinated  $\text{Ni}^{\text{II}}$  complex with thiosemicarbazones did not inhibit the growth of the organisms<sup>[33]</sup>.

### References:

- [1] Gómez-Saiz P, García-Tojal J, Maestro M, et al. *Eur. J. Inorg. Chem.*, **2003**:2123~2132
- [2] Kovala-Demertzi D, Domopoulou A, Demertzis M, et al. *Polyhedron*, **1994**,**13**(12):1917~1925
- [3] Ferrari M B, Fava G, Pelizzi C, et al. *J. Chem. Soc., Dalton. Trans.*, **1992**:2153~2159
- [4] Mendes I C, Moreira J P, Speziali N L, et al. *J. Braz. Chem. Soc.*, **2006**,**17**(8):1571~1577
- [5] Yang Z Y, Wang Y, Wang Y. *Bioorg. Med. Chem. Lett.*, **2007**, **17**(7):2096~2101
- [6] West D X, Swearingen J K, Martinez J V, et al. *Polyhedron*, **1999**,**18**(22):2919~2929
- [7] Tarasconi P, Capacchi S, Pelosi G, et al. *Bioorgan. Med. Chem.*, **2000**,**8**(1):157~162
- [8] Kumar A, Chandra S. *Synth. React. Inorg. Met. Org. Chem.*, **1993**,**23**(4):671~684
- [9] Ackerman L J, Franwick P E, Green M A, et al. *Polyhedron*, **1999**,**18**(21):2759~2767
- [10] Teoh S, Ang S, Fun H, et al. *J. Organomet. Chem.*, **1999**,**580**



- (1):17~21
- [11]Bermejo E, Carballo R, Castineiras A, et al. *Polyhedron*, **1999**, **18**(27):3695~3702
- [12]Yadav P N, Demertzis M A, Kovala-Demertzi D, et al. *Inorg. Chim. Acta*, **2003**,**349**:30~36
- [13]Nomiya K, Sekino K, Ishikawa M, et al. *J. Inorg. Biochem.*, **2004**,**98**(4):601~615
- [14]Sartorelli A C, Moore E C, Zedeck M S, et al. *Biochemistry*, **1970**,**9**(23):4492~4498
- [15]Byrnes R W, Mohan M, Antholine W E, et al. *Biochemistry*, **1990**,**29**(30):7046~7053
- [16]Padhye S, Kauffman G B. *Coord. Chem. Rev.*, **1985**,**63**:127~160
- [17]Mendes I C, Teixeira L R, Lima R, et al. *J. Mol. Struct.*, **2001**, **559**(1~3):355~360
- [18]Marmur J. *J. Mol. Biol.*, **1961**,**3**(1):208~218
- [19]Reichmann M F, Rice S A, Thomas C A, et al. *J. Am. Chem. Soc.*, **1954**,**76**(11):3047~3053
- [20]Sheldrick G M. *SHELXS-97, Program for the Solution of Crystal Structures*, University of Göttingen, Germany, **1997**.
- [21]Sheldrick G M. *SHELXL-97, Program for the Refinement of Crystal Structures*, University of Göttingen, Germany, **1997**.
- [22]Kang S, Chen Z F, Liang H J. *Guangxi Normal Univ. (Natural Science Edition)*, **2002**,**20**(4):75~80
- [23]Ferrari M B, Capacchi S, Reffo G, et al. *J. Inorg. Biochem.*, **2000**,**81**(1):89~97
- [24]Ferrari M B, Capacchi S, Bisceglie F, et al. *Inorg. Chim. Acta*, **2001**,**312**(1~2):81~87
- [25]Afrasiabi Z, Sinn E, Lin W, et al. *J. Inorg. Biochem.*, **2005**,**99**(7):1526~1531
- [26]Matesanz A I, Cuadrado I, Pastor C, et al. *Anorg. Allg. Chem.*, **2005**,**631**(4):780~784
- [27]Pedrido R, Bermejo M R, Romero M J, et al. *Inorg. Chem. Commun.*, **2005**,**8**(11):1036~1040
- [28]Bermejo M R, Gonzalez-Noya A M, Pedrido R M, et al. *Angew. Chem., Int. ED. Engl.*, **2005**,**44**(27):4182~4187
- [29]Bermejo E, Castineiras A, Garcia-Santos I, et al. *Z. Anorg. Allg. Chem.*, **2005**,**631**(11):2011~2019
- [30]Bino A, Cohen N. *Inorg. Chim. Acta*, **1993**,**210**(1):11~13
- [31]Baguley B C, Lebre M. *Biochemistry*, **1984**,**23**(5):937~943
- [32]Lakowicz J R, Webber G. *Biochemistry*, **1973**,**12**(21):4161~4170
- [33]Kasuga N C, Sekino K, Koumo C, et al. *J. Inorg. Biochem.*, **2001**,**84**(1):55~65